Available online at www.sciencedirect.com
SCIENCE DIRECT®
Journal of Power Sources 143 (2005) 166–172
JOURNAL OF POWER SOURCES
www.elsevier.com/locate/jpowsour

Large limits of electrical efficiency in hydrocarbon fueled SOFCs

Roderick W. Sidwell*, W. Grover Coors

CoorsTek R&D Department 4840, 600 Ninth Street Golden, CO 80401, USA

Received 12 November 2004; accepted 9 December 2004
Available online 4 February 2005

Abstract

This paper develops a model for the study of solid oxide fuel cell (SOFC) electrical efficiency. The chemically reacting flow model considers the coupled behavior of fluid mechanics, thermodynamic equilibrium, and transport of electroactive species through the electrolyte. Fuel cells are treated as plug flow tubular reactors with no upstream diffusion. Minimization of free energy is used to calculate gas composition along the length of the fuel channel without specifying a set of reactions. The model serves to place an upper bound on electrical efficiencies. The usefulness of the model is demonstrated by simulating SOFC electrical efficiency as a function of operating voltage for in situ reforming of four different fuel mixtures, including steam reforming and partial oxidation of CH_4, syngas, and pure CH_4.

Keywords: SOFC; Electrical efficiency model; In situ hydrocarbon reforming; Minimization of free energy

1. Introduction

The commercial feasibility of fuel cells rests on the cost of the fuel cell system and operating cost. The latter is determined mostly by electrical efficiency and fuel cost. Anode-supported solid oxide fuel cells (SOFCs) are especially attractive since they are both fuel-flexible and potentially highly efficient [1].

Our paper reports the limiting electrical efficiency of SOFCs as constrained by thermodynamics for three different fuel mixtures and pure CH_4. In situ processing of syngas (66.7% H_2 and 33.3% CO), CH_4 by steam reforming, and CH_4 by partial oxidation are reported. POX is especially attractive since it obviates the need to inject steam into the fuel stream. The model developed here determines the maximum intrinsic electrical efficiency obtainable in a SOFC for any hydrocarbon fuel mixture. The essential question addressed is whether or not ceramic fuel cells can reach electrical efficiencies higher than about 60%, in order to be competitive with utility power [2,3].

Performance of the fuel cell is modeled on the basis of gas composition in the anode channel. Although the gas composition at the cathode is also important, flow in the cathode channel (generally ambient air) is typically many times greater than that in the anode channel. Thus, gas composition along the cathode channel may be treated as constant. With fast chemical kinetics and minimal mass transport limitations, gas in the anode channel will approach the composition predicted by thermodynamic equilibrium. Therefore, ionic transport of the ions (O^{2-}) through the electrodes and electrolyte becomes the rate-determining step in our model.

An advantage of the minimization of free energy method [4] is that it only requires the free energy of reactant and product species. Knowledge of reaction mechanisms or equilibrium constants is not required, a priori. Nonetheless, all major species must be accounted for. Sasaki and Teraoka

* Corresponding author. Tel.: +1 720 838 7566.
E-mail addresses: SidwellRod@comcast.net (R.W. Sidwell); GCoors@CoorsTek.com (W.G. Coors).

0378-7753/$ – see front matter © 2005 Published by Elsevier B.V.
doi:10.1016/j.jpowsour.2004.12.004

[5] examined a wide range of possible SOFC fuels and found five primary fuel cell gases, H_2, H_2O, CO, CO_2, CH_4, as well as graphite. Moreover, they predicted the open circuit potential of the thermodynamic equilibrium mixture in terms of the C–H–O ratio and used Gibbs minimization to calculate equilibrium gas mixtures. In a kinetic study of steam reforming of methane and water gas shift (WGS) reactions on a $Ni/MgAl_2O_4$ catalyst, Xu et al. [6] proposed an 11-reaction mechanism, which included the same five gas-phase species reported by Sasaki and Teraoka.

Demin et al. [7,8] developed a thermodynamic model for estimating the system efficiency, including electrical efficiency, of SOFCs operating on steam–methane mixtures. Their model developed an algorithm for computing the gas composition along the anode channel. The algorithm assumes the same gas phase species as Sasaki and Teraoka and Xu et al. and, unlike our model, assumes two reactions: steam reforming reaction and water gas shift. An important distinction between the Demin et al. models and our model is that they use the average EMF to compute electrical efficiency and assume that all processes occur under reversible conditions, i.e. no load. In contrast, our model calculates the power generated at each point in the cell from the operating voltage and local current. We assume the zero current condition only at the end of the cell. Since our model includes ohmic losses, electrical efficiencies reported in this paper are, therefore, more realistic.

Accounting for high mass transport resistance in the anode support and slow surface chemistry requires a more complex model. Moreover, inclusion of these effects also requires detailed knowledge of the porosity and permeability of the anode support together with well-developed surface reaction mechanisms. Zhu et al. developed a SOFC model which includes both channel flow and porous media flow coupled with heterogeneous surface chemistry in the anode support [9,10]. In Fig. 9 of the paper, Zhu et al. [10] compared gas composition and current densities along the anode channel assuming either heterogeneous kinetics or chemical equilibrium. In the range of interest where commercial fuel cells are operated, that is, at high thermodynamic and Faradaic efficiency, both kinetic and equilibrium models predict nearly equivalent fuel cell performance.

A difficulty with kinetic models is that the validity of the predictions depends on detailed a priori knowledge of rate constants. Such knowledge is often not available for the conditions of interest. In the present model, gas in the anode channel is assumed to be at chemical equilibrium along the entire length of the fuel cell. Moreover, by providing an arbitrarily long fuel cell, the fuel cell is able to reach reversible conditions (zero current) by the time the fuel exits the cell. We do not seek to replace kinetic models. Instead, our model serves to establish an upper bound of electrical efficiency based on the Second Law rather than complex overpotentials which are fuel cell specific and, in many cases, poorly understood.

2. Model development

Composition of the gas flow in the anode channel depends on the coupled behavior of fluid mechanics, thermodynamic equilibrium, and transport of electroactive species through the electrolyte. Gases in the anode channel are treated as a plug flow (radially well-mixed with no axial diffusion). For the very low flow rates considered here (velocities of the order of $3\,cm\,s^{-1}$ and Reynolds number 10), pressure losses are insignificant over the length of the tube. Gas pressure and temperature in both anode and cathode channels is assumed to be isobaric and isothermal.

Fig. 1 illustrates two arrangements for anode-supported fuel cells. Fuel mixtures flow through the interior anode channels. Air flows around the outside of the tube (left) or through the bottom channel (right). On the left side of Fig. 1, the channel is cylindrical and the electrolyte extends around the entire perimeter. For the cylindrical tubes, the fuel cell stack consists of multiple tubes connected to a fuel manifold. For the planar configuration (right side Fig. 1), three of the walls are metal interconnects.

The anode support and electrolyte boundary occupy the bottom of the anode channel. Although our model is developed for tubular geometry, it is general, and may be applied to other configurations where the cross-section perpendicular to flow and electrolyte area are known.

The anode support, typically Ni/8YSZ cermet, is a good electrical conductor and each tube operates at a single voltage, V_{cell}.

Transport of O^{2-} ions from cathode to anode alters the local gas composition along the anode channel by oxidizing the fuel. For a sufficiently long tube, the extent of fuel oxidation depends on the cell operating voltage, V_{cell}. As the mixture becomes oxidized, the reversible voltage, E_r, drops until it reaches V_{cell}. Beyond this point, additional ionic current cannot flow, and it is not possible to oxidize the fuel any further. Faraday's Law relates the local molar

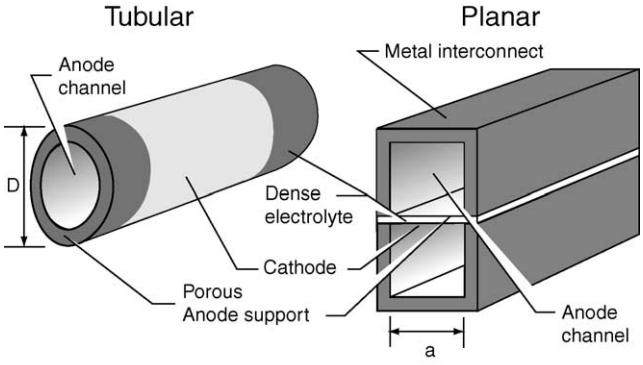

Fig. 1. Anode-supported SOFCs. Left, a tubular arrangement where the entire tubular anode support is covered with electrolyte; right, a square channel arrangement where one side of the channel is covered with electrolyte.

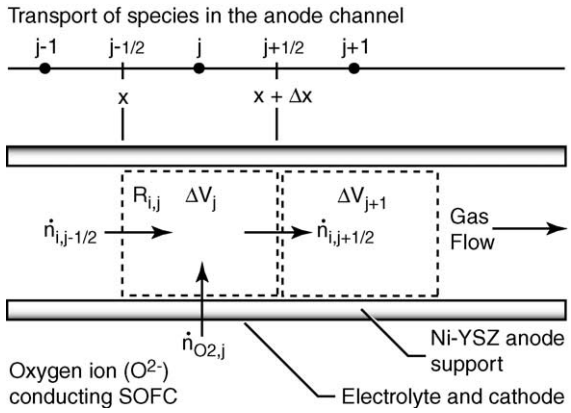

Fig. 2. The fuel cell is modeled as a plug flow reactor with no upstream diffusion. The gas entering each volume element reaches chemical equilibrium.

flow of O^{2-} ions through the electrolyte to the local electric current,

$$i = z_e F \frac{dn}{dt}, \tag{1}$$

where i is in A, $z_e = -2$ the charge transfer per ion, F Faradays constant, and n is moles of O^{2-} ions.

Our model uses a shell balance to segment the tube into discrete volume elements. Fig. 2 represents the shell-balance control volumes of elements j and $j+1$. Three control surfaces account for transport of species into each control volume. A mole balance of species i entering, leaving, reacting, and/or accumulating within a control volume is shown in Fig. 2, where $\dot{n}_{i,j-1/2}$ is the molar flow of species i into the element j, $R_{i,j}$ the rate of creation or annihilation of species i caused by chemical reactions in element j, $\dot{n}_{O_2,j}$ the molar flow of O_2 due to transport of O^{2-} ions through the electrolyte, and $\dot{n}_{i,j+1/2}$ is the molar flow out of element j. For the steady state case, the net rate of accumulation, dn_{ij}/dt, is zero for all species.

Summing over all the species, N, in element j, at steady state, the molar flows in Fig. 2 become,

$$\sum_{i=1}^{N} \dot{n}_{i,j-1/2} + \dot{n}_{O_2,j} - \sum_{i=1}^{N} \dot{n}_{i,j+1/2} + \sum_{i=1}^{N} R_{i,j} = 0. \tag{2}$$

Eq. (2) is a form of the general mole balance equation, which is described elsewhere [11]. We assume that the molar flow into each volume element, $\dot{n}_{i,j-1/2}$, immediately reaches equilibrium upon entering the control volume. Chemical reactions create and/or destroy species to reach equilibrium composition, which is calculated by Gibbs minimization. Chemical equilibrium itself depends upon gas composition, temperature T, and pressure P. To reach chemical equilibrium, the rate at which each specie is created or destroyed must be equal to the difference between the non-equilibrium flow coming into the control volume and the equilibrium mixture flow,

$$\sum_{i=1}^{N} R_{i,j} = \sum_{i=1}^{N} \dot{n}_{eqi,j} - \sum_{i=1}^{N} \dot{n}_{i,j-1/2}, \tag{3}$$

where positive $R_{i,j}$ represents creation of species i and negative $R_{i,j}$ represents annihilation of species i. The rate of fuel oxidation depends on the rate of transport of O^{2-} ions through the electrolyte. Nevertheless, we can immediately find the equilibrium composition in each element j as a function of the amount of O_2 added to the anode channel. Our model relies on HSC software [12] to minimize the Gibbs free energy in each volume element (Eq. (3)). Combining Eqs. (2) and (3) yields,

$$\sum_{i=1}^{N} \dot{n}_{eqi,j} + \dot{n}_{O_2,j} = \sum_{i=1}^{N} \dot{n}_{i,j+1/2}, \tag{4}$$

which is the non-equilibrium molar flow leaving volume element j and entering element $j+1$. Thus, the calculation proceeds in a marching fashion from the channel inlet, $j = 1$, to the last volume element of the cell, $j = L$.

Generally, moles are not conserved in the control volume due to chemical reactions and net addition of O_2 through the electrolyte. As a result, gas velocity increases along the length of the tube. For an ideal gas, the velocity of the gas into element j is stated as,

$$\langle v_{j-1/2} \rangle (\mathrm{cm\,s^{-1}}) = 22414 (\mathrm{cm^3\,mol^{-1}}) \times \frac{T}{273} \frac{P_0}{P} \frac{\sum_{i=1}^{N} \dot{n}_{i,j-1/2} (\mathrm{mol\,s^{-1}})}{A(\mathrm{cm^2})}, \tag{5}$$

where T is temperature (K), P pressure, $\dot{n}_{i,j-1/2}$ molar flow of species i through the control surface at $j - 1/2$, N the total number of species, and A is the cross-sectional area of the channel.

In each element j, the equilibrium gas composition is perturbed by the transport of O^{2-} ions through the electrolyte. Combining Ohms Law and Eq. (1), the current produced by a SOFC volume element is,

$$i_j = \frac{E_{r,j} - V_{cell}}{R_{ohm,j}} = 4F\dot{n}_{O_2,j}, \tag{6}$$

where V_{cell} is the cell voltage, $2 \times z_e = 4$ the charge transfer for a O_2 molecule, $R_{ohm,j}$ the apparent electrical resistance of the element, F Faradays constant, and $\dot{n}_{O_2,j}$ is the molar flow of O_2. The reversible voltage for element j in Eq. (6) is,

$$E_{r,j} = E_j^0 + \frac{RT}{4F} \ln(P_{O_2}(c)) + \frac{RT}{2F} \ln\left(\frac{P_{H_2,j}(a)}{P_{H_2O,j}(a)}\right). \tag{7}$$

where c and a indicate partial pressures at the anode and cathode, respectively. The reversible voltage of the cell depends on the equilibrium potential between the electrodes, and is taken as the open circuit voltage of element j. The operat-

ing voltage of the cell, V_{cell}, must be less than the reversible voltage, E_{r}, for current to flow spontaneously.

As an electrical load is applied to a fuel cell, the voltage across the electrolyte can be represented most generally as,

$$V_{\text{cell}} = E_{\text{r}} - \eta_{\text{conc,a}} - \eta_{\text{a}} - \eta_{\text{ohm}} - \eta_{\text{conc,c}} - \eta_{\text{c}} - \eta_{\text{interface}} - \eta_{\text{leakage}}, \quad (8)$$

where $\eta_{\text{conc,a}}$ and $\eta_{\text{conc,c}}$ are the concentration overpotentials at the anode and cathode due to diffusion resistance, η_{a} and η_{c} the activation polarizations at the anode and cathode, η_{ohm} the ohmic polarization, $\eta_{\text{interface}}$ represents surface polarization phenomena, and and η_{leakage} is the polarization loss due to electron leakage [9]. For the model presented here, we lump all of the linear polarization phenomena into the ohmic polarization term η_{ohm} and discard all non-linear polarization effects. Activation polarizations, which do not depend on current, are assumed to be much smaller than η_{ohm}, and are not considered. Consequently, the current–voltage (*IV*) characteristic curve is treated as a straight line, and each $R_{\text{ohm},j}$, in units of ohms, is constant within each element *j*. For the isothermal conditions investigated here, the area-specific resistance (ASR), in units of $\Omega\,\text{cm}^2$, is constant for all volume elements.

Fig. 3 illustrates *IV* curves for two adjacent volume elements *j* and $j+1$. Each element *j* has its own reversible voltage determined from the gas composition in the volume element. The upper curves represent element *j*, which has a higher reversible voltage E_{r}. A short distance down the channel, element $j+1$, the reversible voltage is lower and the *IV* curve is shifted.

The excess potential ΔV_j is equal to the difference between the reversible voltage, $E_{\text{r},j}$, and the cell voltage, V_{cell}. Ohms Law holds for each volume element and the excess voltage, ΔV, is related to the current i_j by,

$$\Delta V_j = E_{\text{r},j} - V_{\text{cell}} = i_j R_{\text{ohm},j}, \quad (9)$$

where i_j and $R_{\text{ohm},j}$ (units of ohms) are the current and electrical resistance of volume element *j*, respectively. The resistance in each element, which depends on the ASR and electrolyte area contacting the gas in the anode channel, is stated as,

$$R_{\text{ohm},j} = \frac{\text{ASR}}{\pi D \Delta x_j}, \quad (10)$$

where $\pi D \Delta x_j$ is the wetted electrolyte area A_j (see Fig. 1).

Both top and bottom panels in Fig. 3 show ohmic losses in each element as a dark shaded triangular region above the cell voltage V_{cell}. The power in each element *j* is shown as square shaded regions below the operating voltage V_{cell}. Importantly, Fig. 3 shows that the electrical power of every element *j* includes all ohmic losses.

Consider two alternatives to calculate the molar flow of O_2, $\dot{n}_{O_2,j}$, into each volume element. We could fix Δx_j, (making the volume and electrical resistance of each segment the same, see Fig. 2) and solve for the current

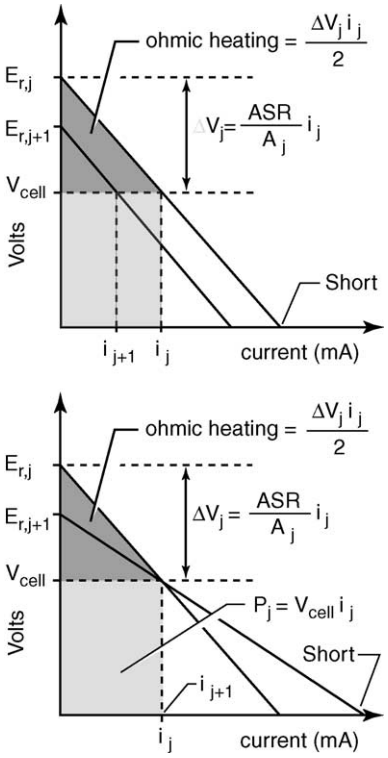

Fig. 3. Each segment along the length of the fuel cell tube has its own *IV* curve; curves for *j* and $j+1$ are shown here. In the top panel, the length of each volume element Δx_j and resistance is held constant for all elements. The lower panel shows the *IV* curves for adjacent elements with constant current. In both top and bottom panels, the ASR is constant.

by means of Eq. (6). Alternatively, we could add a constant amount of O_2 to each volume element, and allow the segment length to vary. The next sections discuss each approach.

2.1. Dimensional solution

The current and molar flow of O^{2-} ions in each volume element will vary with the excess potential, ΔV_j, while the electrical resistance remains fixed. The solution is then achieved in a marching fashion from the inlet to the outlet in steps of Δx. Importantly, this approach requires fuel cell specific geometrical information, tube diameter, ASR, electrolyte area (through Eq. (10)), and operating conditions.

As shown in the top panel of Fig. 3, the slopes of the *j* and $j+1$ curves are equal since the electrical resistance in each element is constant. As fuel in the anode channel is consumed, a family of parallel *IV* curves is formed, each shifting downwards as the reversible voltage, E_{r}, drops. Current in each segment is found from the intersection of V_{cell} and the *IV* curve. Ideally, $E_{\text{r},j} = V_{\text{cell}}$ in the final element ($j = L$) and the current is zero. In practice, the reversible voltage drops very rapidly as the fuel nears complete oxidation and the final element is identified as last element having positive excess voltage ΔV_j.

2.2. Dimensionless solution

In the dimensionless approach, the molar flow of O_2 into each element is fixed and we solve for the reversible voltage $E_{r,j}$ of each element j. From Faradays Law, Eq. (1), it can be seen that current, i_j, and molar flow of oxygen, $\dot{n}_{O_2,j}$, are proportional.

In the bottom panel in Fig. 3, the molar flow of O_2 into each element, $\dot{n}_{O_2,j}$, is fixed. The length of each element, Δx_j, changes to adjust the element resistance and maintain a fixed current. As fuel is consumed the reversible potential, E_r, drops and the *IV* curve rotates. A family of *IV* curves, which pivot about a single point, are formed. Ideally, in the last element, the reversible voltage E_r reaches the cell voltage V_{cell} and the resistance reaches zero. Numerically, the end of the cell is reached when a discrete addition of O_2 results in a negative excess potential ΔV and the slope of the *IV* curve becomes positive.

The equilibrium gas composition and reversible voltage along the fuel cell is known as a function of O_2 added per mole of inlet fuel mixture, i.e. the extent of the oxidation reaction. Moreover, the stoichiometric amount of O_2, needed to fully oxidize the inlet mixture, is also known. Therefore, the problem can be scaled on a molar basis, with the amount of O_2 added to the inlet mixture ranging from zero to stoichiometric (as a practical matter, accuracy of the solution may be improved by adapting the step size of $\dot{n}_{O_2,j}$ to the rate of change of the reversible voltage E_r). For a given operating voltage, V_{cell}, both the excess potential, ΔV, and total current are also known. With reversible voltage, total current and fuel flow in hand, the electrical efficiency is easily calculated, and is defined as,

$$n_e = \frac{P_{total}}{\sum_{i=1}^{N} \dot{n}_i \Delta H_i} \tag{11}$$

where P_{total} is the total electrical power, $\dot{n}_i$ the inlet molar flow rate of fuel species i per mole of total gas flow at the inlet, N the number of fuel species, and ΔH_i is the enthalpy for complete oxidation of species i. The operating voltage is constant, the electrical power from a single volume element j is,

$$P_j = i_j V_{cell}. \tag{12}$$

Therefore, the total electrical power for the fuel cell is,

$$P_{total} = 4FV_{cell} \sum_{j=1}^{L} \dot{n}_{O_2,j}, \tag{13}$$

where F is Faradays constant, $\dot{n}_{O_2,j}$ the molar flow of O_2 into each element j, and L is the last volume element with a positive excess potential ΔV. The electrical efficiency (Eq. (11)) becomes,

$$\eta_e = \frac{4FV_{cell} \sum_{j=1}^{L} \dot{n}_{O_2,j}}{\sum_{i=1}^{N} \dot{n}_i \Delta H_i}. \tag{14}$$

The total channel length is found by,

$$L_{total} = \sum_{j=1}^{L} \Delta x_j, \tag{15}$$

where L is the number of volume elements and Δx_j is the length of element j. Of course, Δx_j goes to infinity as the excess potential ΔV_j and current density approach zero. Therefore, a small ΔV must be chosen to truncate the solution.

Since the electrical efficiency of the fuel cell depends only on temperature, composition, and operating voltage, a more general, dimensionless, solution to the problem is obtained. The general solution may then be used to calculate the length of each volume element based on fuel cell specific information, i.e. ASR, channel cross-section, electrolyte area per unit length, and molar flow at the inlet.

The current per mole of inlet flow of each element j is used to scale the solution to the specific geometry (see Fig. 1) of a particular fuel cell. For a fixed value $\dot{n}_{O_2,j}$, the length of the volume element, Δx, changes to accommodate the varying current density. Thus, the length of each volume element Δx_j is needed to scale the solution. Both the molar flow of O_2 and excess voltage are known and the length of volume element j is found as,

$$\Delta x_j = \frac{\mathrm{ASR}}{\pi D} \frac{4F\dot{n}_{O_2,j}}{(E_{r,j} - V_{cell})}. \tag{16}$$

Eq. (16) together with $E_{r,j}$ is used to calculate current densities and power profiles. From the equilibrium gas composition of each element j, one may obtain mole fraction and velocity profiles inside the anode channel (Eqs. (6) and (16)).

3. Results and discussion

Our model can be applied to a wide range of fuel cell conditions to provide useful insight into various design fueling options. In the following example, different methods of processing methane are considered.

Fig. 4 shows the electrical efficiency as a function of operating voltage for four different inlet mixtures (composition in mole fractions), pure CH_4, POX (0.408 CH_4, 0.123 O_2, 0.059 H_2O, and balance N_2), syngas (0.667 H_2 and 0.333 CO), and steam reforming (0.667 H_2O and 0.333 CH_4). Syngas composition varies depending on the hydrocarbon source. The 2:1 H_2:CO ratio represents the inlet fuel composition one would expect from steam reforming a 50/50 mixture CH_4 and coal at high temperature. In all cases, temperature is isothermal and maintained at 800 °C.

Pure CH_4 (triangles) is shown to give a bounding case and results in the highest electrical efficiency, 75%. In practice, pure CH_4 cannot be used because of coke formation. The maximum electrical efficiency for the partial oxidation case, 63% at 814 mV, is considerably lower than that for steam reforming, 72.7% at 797 mV (shown with squares). Syngas (shown with crosses) yields the lowest electrical efficiency,

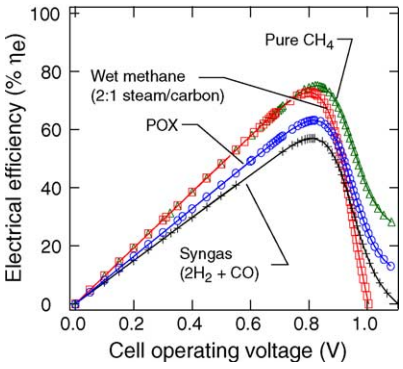

Fig. 4. SOFC electrical efficiency as a function operating voltage for four different gas mixtures. Temperature is maintained at 800 °C and pressure is 1 bar.

57% at 815 mV. As shown, steam reforming results in a lower open circuit voltage and higher electrical efficiency than either syngas or POX. An important finding from the model is that both internal steam reforming and POX can be employed in fuel cells with >60% electrical efficiency while the use of 2:1 syngas cannot.

Consider the low efficiency regions in Fig. 4. For operating voltages ranging from zero to around 700 mV efficiency responds linearly with the operating voltage because oxidation of the fuel is nearly complete. This is a region characterized by high fuel efficiency (Faradaic efficiency) but low thermodynamic efficiency. A second region of low efficiency occurs at high operating voltages. High operating voltage prevents full oxidation of the fuel, which results in low electrical current per mole of incoming fuel. This region is characterized by high thermodynamic efficiency but low Faradaic efficiency. At peak electrical efficiency, a compromise between operating voltage and fuel utilization is made. Operation at peak efficiency results in considerable fuel slip. For the steam reforming case, the exhaust gas at peak efficiency contains 3.4 vol% H_2, while POX exhausts 3.3 vol% H_2 (or 0.14 moles H_2 exhausted per mole CH_4 feed), and syngas results in 4.0 vol% H_2 in the exhaust.

The thermodynamic limit of fuel utilization for any operating voltage V_{cell} is reached when $V_{cell} = E_r$, i.e. current will not flow spontaneously unless the operating voltage is below the reversible voltage. Once $V_{cell} = E_r$, no current is drawn and gas composition in the anode channel does not change. Clearly, one cannot arbitrarily increase the cell operating voltage to increase electrical efficiency. An important finding is that, high open circuit voltages, while desirable, should not be used to infer high electrical efficiency.

4. Conclusions

In the spirit of Carnot efficiency for heat engines, we have developed a numerical model which predicts the theoretical electrical efficiency for SOFCs. Since Gibbs minimization is used to calculate gas composition, any fuel mixture may be considered without a priori knowledge of the chemical reactions involved. The model assumes that the cell length is sufficiently long for gas composition in the anode channel to reach equilibrium with the Nernst potential ($E_r = V_{cell}$) at the outlet.

When a second assumption holds, i.e. transport of ions through the electrolyte is the rate limiting step, the model is able to predict conditions along the length of a SOFC anode channel. These conditions include:

- current density and power profiles;
- gas phase mole fraction profiles;
- fuel slip as a function of cell length, operating voltage, or changing inlet flow;
- minimum fuel cell length for a given electrical efficiency.

SOFCs promise exceptional efficiency when operated appropriately. Nonetheless, our results show that one cannot arbitrarily increase the operating voltage to increase electrical efficiency. Peak electrical efficiency is a compromise between fuel utilization and operating voltage, which are antagonistic. We also find that high open circuit voltage is not necessarily a good indicator of high electrical efficiency. We conclude that it is possible to exceed 60% electrical efficiency in internally reforming SOFCs. We also conclude that, all things considered, POX may provide adequate efficiency for many SOFC applications.

References

[1] EG&G Technical Services Inc. and Science Applications International Corporation (Eds.). Fuel Cell Handbook (sixth ed.), U.S. Department of Energy Office of Fossil Energy National Energy Technology Laboratory, 2002.
[2] W.G. Coors, Development of a protonic ceramic fuel cell at Protonetics, in: J. Huijsmaus (Ed.), Proceedings of the Fifth European SOFC Forum, 2002, pp. 602–607.
[3] G. Coors, R. Sidwell, F. Anderson, Characterization of electrical efficiency in proton conducting fuel cells, in: M. Morgensen (Ed.), Proceedings of the European Solid Oxide Fuel Cell Forum, vol. 1, 2004, pp. 117–124.
[4] S. Gordon, B.J. McBride. Computer program for the calculation of complex chemical equilibrium compositions and applications. Part I. Analysis. Reference publication 1311, NASA, 1994.
[5] K. Sasaki, Y. Teraoka, Equilibria in fuel cell gases, Electrochemical Society Proceeding, SOFC VIII, 2003, pp. 1225–1239.
[6] J. Xu, G.F. Froment, Methane steam reforming, methanation and water-gas shift. Part I. Intrinsic kintics, AIChE J. 35 (1) (1989) 88–96.
[7] A.K. Demin, V. Alderucci, I. Ielo, G.I. Fadeev, G. Maggio, N. Giordano, V. Antonucci, Thermodynamic analysis of methane fueled solid oxide fuel cell system, Int. J. Hydrogen Energy 17 (6) (1992) 451–458.
[8] A.K. Demin, P.E. Tsiskaras, V.A. Sobyanin, S.Yu. Hramova, Thermodynamic analysis of a methane fed SOFC system based on a protonic conductor, Solid State Ionics 152–153 (2002) 555–560.

[9] H. Zhu, R.J. Kee, A general mathematical model for analyzing the performance of fuel-cell membrane-electrode assemblies, J. Power Sources 117 (2003) 61–74.
[10] H. Zhu, R.J. Kee, V.M. Janardhanan, O. Deutschmann, D.G. Goodwin, A computational model for coupled fluid flow, porous-media transport, heterogeneous chemistry, and electrochemistry in solid-oxide fuel cells, J. Electrochem. Soc., submitted for publication.
[11] H. Scott Fogler, Elements of Chemical Reaction Engineering, Prentice Hall PTR, Upper Saddle River, NJ 07458, 1992.
[12] Outokumpu Research, Outokumpu HSC Chemistry for Windows, Version 5.1 ed.